Proton Magnetic Resonance Imaging of Lipid in Pecan Embryos

John M. Halloin[a,*], Thomas G. Cooper[b], E. James Potchen[b] and Tommy E. Thompson[c]

[a]Sugarbeet, Bean and Cereal Research Unit, ARS, USDA and Department of Botany and Plant Pathology, Michigan State University, East Lansing, Michigan 48824, [b]Department of Radiology, Michigan State University and [c]Pecan Breeding and Genetics Station, ARS, USDA, Somerville, Texas 77879

Magnetic resonance images of plant tissues typically are manifestations of water protons in tissues. Within oilseeds, however, lipids contain a major portion of the mobile protons, which should enable specific imaging of lipids. In this study, experiments were done to demonstrate spin-echo imaging (SEI) and chemical-shift imaging (CSI) of lipid within nonimbibed and imbibed embryos of pecan (*Carya illinoensis*), a high-lipid seed. Magnetic resonance spectra of air-dry embryos contained a single major peak for lipid, whereas those of imbibed embryos contained separate peaks for water and lipid. This separation of spectral peaks enabled CSI of distributions of either lipids or water in imbibed embryos. A longer spin-spin relaxation time of lipid protons than of water protons in imbibed embryos allowed selective SEI of lipids in those embryos. SEI of normal, dry embryos revealed fairly uniform distribution of lipids across tissues. Similar images of embryos damaged by the fungus *Phoma exocarpina* or the insect *Zerara viridula* were less intense than those of a normal embryo, reflecting the lower oil contents of the damaged embryos. Magnetic resonance imaging should provide a useful technology for studying lipid distribution and metabolism within oil seeds.

KEY WORDS: *Carya illinoensis*, magnetic resonance imaging, NMR spectroscopy, oilseeds, seed decay.

Proton magnetic resonance imaging (MRI) has attained widespread use as an important tool in medical diagnostics. It has the advantage of yielding high-quality images without ionizing radiation. The methods are nondestructive and noninvasive. Increased availability of this technology has led to its increasing use as a tool for plant research in a diverse array of systems (1–8). Because water is the most abundant source of imageable protons (^{1}H nuclei) in most plant tissues, all plant proton MRI studies to date have involved the imaging of water protons and variations in their abundances and interactions with their molecular environments. The methods, however, are capable of producing images of any resonating protons that are sufficiently abundant to provide detectable signals. There are many proton sources within plant tissues that would not be excluded by bandwidth in conventional MRI experiments. However, most of these protons lack sufficient mobility to have relaxation times long enough for imaging. The greater freedom of rotation of water protons results in relaxation times that allow detection by MRI techniques. Because the lipids in seeds of high oil content contain numerous protons, MRI should be applicable to imaging of lipid distribution within those seeds. This study demonstrates the application of two MRI techniques to imaging of lipid distribution within embryos of pecan [*Carya illinoensis* (Wangenh.) K. Koch], a high oil content seed (9). Images of lipid in pecan embryos were included among some of the earliest MRI studies (10), but they provided little of the resolution or the variations in contrast that are attainable today.

*To whom correspondence should be addressed.

The two imaging techniques used in this study, chemical-shift (CSI) and spin-echo imaging (SEI), although sometimes yielding similar images, differ in the types of information that they provide. CSI provides information on the abundance of particular classes of nuclei, comparable to that achieved in nuclear magnetic resonance (NMR) spectra, but with two spatial dimensions added to provide a two-dimensional image. The third dimension, perpendicular to the plane of the image, contains spectral information on the entire sample at a particular point in space, and thus reflects proton abundance [N(H)] within the entire sample at that point, shown as image intensity (11). SEI, like CSI, is dependent not only upon N(H), but also upon physical characteristics (relaxation) of protons in magnetic fields, known as spin-lattice (T1) and spin-spin (T2) decay (12). SEI images, while providing the two-dimensional appearance of CSI, have a spatial third dimension, thickness. Intensity at any point on the image is a manifestation of interactions between N, T1 and T2, as well as imaging parameters used in the instrument.

EXPERIMENTAL PROCEDURES

Pecans purchased from a local merchant were shelled, and the embryos were separated into three groups: Normal; rotted by a fungus identified as *Phoma exocarpina* Pk; and a group with dark brown mottling, the apparent result of damage by green stink bugs (*Zerara viridula* L.; Ref. 13). The latter two groups each comprised approximately 3–4% of the total sample. Another sample was obtained at a later time for use in studies on CSI.

Cotyledons (half embryos) were placed on moistened filter paper in petri dishes for 24 h at 22°C for imbibition. These cotyledons and nonimbibed embryos were weighed and then dried to constant weight at 105°C for moisture determinations. Another group of embryos was weighed, ground in a mortar and pestle under liquid nitrogen and extracted with hexane in a Soxhlet apparatus. The resulting hexane/oil solution was evaporated to remove hexane, and the residual oil was weighed. Oil samples from normal pecans were used for magnetic resonance spectral and proton relaxation determinations.

The magnetic resonance T1 and T2 relaxation constants and spectra were measured, and images were acquired with a 4.7-Tesla General Electric Omega CSI system (General Electric Corp., Fremont, CA). The receiving coil, a General Electric 6-inch bird cage coil, was tuned and matched, and the magnet was shimmed with each sample to provide maximum magnetic field homogeneity. Data analysis was done with a SUN 3/160-based computer. Relaxation constants were measured by conventional (14) repetitive inversion recovery (for T1) and spin-echo (for T2) determinations; echo intervals varied among samples. The data acquisition matrix for SEI was 256 in the frequency-encoded direction by 128 in the phase-encoded direction, with zero filling to 256 × 256 prior to Fourier transformation. Spin-echo sequence repetition times (TR), echo times (TE), slice thicknesses (ST), numbers of acquisitions (NA) and total imaging times (IT)

for samples varied, and were as follows for the three spin-echo images presented later in the paper: Figure 2C, TR = 0.5 s, TE = 20 ms, ST = 1 cm, NA = 4 and IT = 8 min, 32 s; Figure 3A, TR = 0.5 s, TE = 16 ms, ST = 2 mm, NA = 4 and IT = 8 min, 32 s; and Figure 3C, TR = 0.5 s, TE = 16 ms, ST = 1 mm, NA = 8 and IT = 17 min, 4 s. In data acquisition for CSI (11), we employed a matrix of 64 × 64 in the phase-encoded dimensions, with a spectral width of 5000 Hz. Spectral data were accumulated as 256 data sets, each representing *ca.* 19.5 Hz. Repetition time was 0.5 s, with 2 acquisitions, and an IT of 68 min, 16 s. Spectral maxima for water and oil were contained in data sets at 3.7 and 0 ppm, respectively.

RESULTS

The NMR spectrum of an imbibed pecan embryo (Fig. 1) showed separation of water and oil peaks by approximately 3.7 ppm, which allowed separation by 22 data sets for CSI. Small amounts of water in air-dry embryos (Tables 1 and 2) were not evident in spectra because they were masked by the large oil peaks. Water in imbibed embryos was relatively tightly bound, as evidenced by the relatively short relaxation constants (Table 1). Oil in air-dry embryos exhibited shorter relaxation constants than free oil, indicating the presence of important binding interactions between oil and any surrounding matrix, despite the fact that such lipid deposits are likely to be localized in discrete vesicles (15). Increases in oil relaxation constants upon imbibition indicate a decrease in these binding interactions upon tissue hydration.

The CSI of oil and water (Figs. 2A and 2B, respectively) in a cotyledon reveal nonuniformity in the distributions of these materials. Because CSI encompasses the entire thickness of the sample, variations in image intensity are partly attributable to variations in subject thickness. ST for the SEI of this cotyledon (Fig. 2C) was set at 1 cm, so as to encompass the entire cotyledon, thereby providing an image comparable in proton abundance to those obtained with CSI. Although SEI is dependent both upon the water and the oil protons in this sample, the interaction of relaxation constants (Table 1) and imaging parameters was such (see Discussion section) that the image is almost entirely reflective of the distribution and physical interactions of oil. Images of the tubes of water and oil in Figure 2 reveal slight signal from oil in the water image (Fig. 2B), but none from the water in the oil image. The absence of the water tube from the SEI is due to radio frequency saturation of water, the result of interactions between the long T1 relaxation of pure water (Table 1) and the imaging parameter TR.

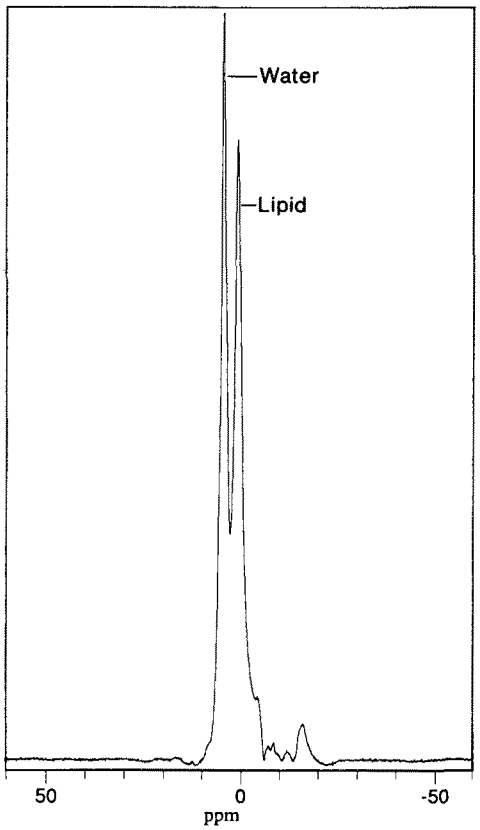

FIG. 1. Proton magnetic resonance spectrum of imbibed pecan embryo showing major peaks for water (left) and for oil (right).

Rotted and insect-damaged embryos were lower than normal embryos, both in fresh weight and oil content, with

TABLE 1

Moisture Contents, Proton Spin-Lattice (T1) and Spin-Spin (T2) Relaxation Constants, and Resonance Frequencies of Samples Used in Magnetic Resonance Imaging Experiments

Sample	Moisture content (%)[a]	Relaxation constant (milliseconds)		Resonance frequency (MHz)
		T1	T2	
Water	na[b]	2814	2043	200.112911
Pecan oil	na	344 (5)[c]	64 (2.5)	200.111282
Air-dry pecan	3.4 (0.2)	283 (12)	22 (0.2)	200.111852
Imbibed pecan	36.8 (1.9)	na	na	na
Oil peak	na	439 (42)	32 (0.9)	200.111559
Water peak	na	261 (34)	14 (1.3)	200.112246
LSD (0.05)[d]	4.5	76	5	0.000196

[a]Moisture as a percentage of fresh weight.
[b]na, Not applicable.
[c]Values in parentheses are standard errors of the means.
[d]All values are means of four replicate samples; LSD (least significant difference) values are exclusive of determinations for free water.

TABLE 2

Fresh Weights, Moisture and Oil Contents of Normal Pecans and Those Rotted by the Fungus *Phoma exocarpina* or Injured by the Insect *Zerara viridula*

Sample	Fresh weight (g)	Moisture content (%)	Oil content (%)
Normal	3.19	1.8	62.5
Rotted	2.04	3.5	39.7
Insect-damaged	2.63	2.4	55.4
LSD[a] (0.05)	0.53	0.6	4.7

[a]Least significant difference.

rotted ones being lowest in both categories (Table 2). The embryos selected were similar in size, so obviously there would be fewer oil protons present per unit volume of tissue. This relationship is apparent in the MRI of these embryos (Fig. 3A), with the image of the rotted embryo being faint in comparison with the normal one. Signal intensity in images of the insect-damaged embryo (Figs. 3A, right, and 3C) appeared more intense in areas not exhibiting dark surface mottling (the lower, right portion of the cotyledon, Fig. 3B), but was quite uniform in cross sections of the other embryos.

DISCUSSION

The interaction between the sample characteristics N(H), T1 and T2, and the instrument settings TR and TE, to determine image intensity (I) at any point in an image is described by the formula: $I = N(H)(1 - e^{-TR/T1})e^{-TE/T2}$ (12). Peak areas for water and lipid in NMR spectra of imbibed embryos tended to be similar, indicating similar numbers of water protons and C-bonded oil protons in the samples. Use of the above formula, relaxation constants from Table 2, the instrument parameters used for Figure 2C, and assumption of proton equality between water and oil leads to the determination that more than 90% of the signal shown in that SEI is due to lipid. This weighting of the image results from the more than twofold difference in T2 values between the two components, and the proportion of oil signal in the image could be increased by increasing TE. Thus, either CSI or SEI can be used to image lipid distribution in either dry or imbibed embryos.

The methods used in this study should be applicable to studies of lipid distribution and metabolism in other oilseeds and potentially may prove useful for mass screening of seeds for exceptional variations in lipid content. Similar SEI studies, coupled with spectroscopy, were used to study localization and metabolism of lipids during development of an insect (16). Each of the imaging techniques has its advantages and disadvantages for imaging of seed lipids. CSI provides data that are dependent upon proton abundance and chemical bonding, whereas SEI provides data that are influenced by nuclear interactions with surrounding molecules. Resolution in the plane of the image can be comparable for the two methods, but requires much more imaging time with CSI than with SEI; to provide comparable resolution with CSI in Figure 2A to that shown with SEI in Figure 2C would have required approximately 18.2 h *vs.* approximately 8.5 min. SEI provides image slices of uniform thickness, whereas

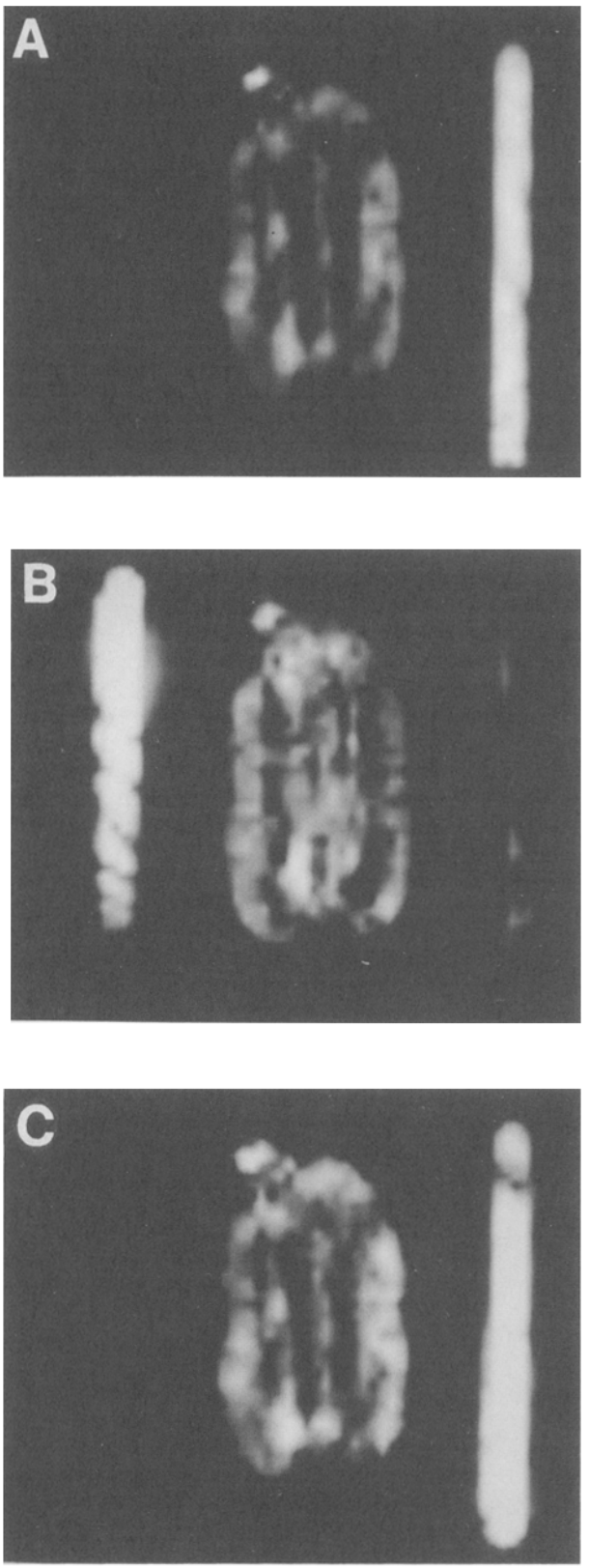

FIG. 2. Chemical-shift images of an imbibed pecan cotyledon at the oil (A) and water (B) frequencies, and a spin-echo image (C) of the same cotyledon. The bars on either side of the cotyledon are tubes containing either water (left) or pecan oil (right). The spin-echo image has a slice thickness of 1 cm, so as to contain the entire cotyledon.

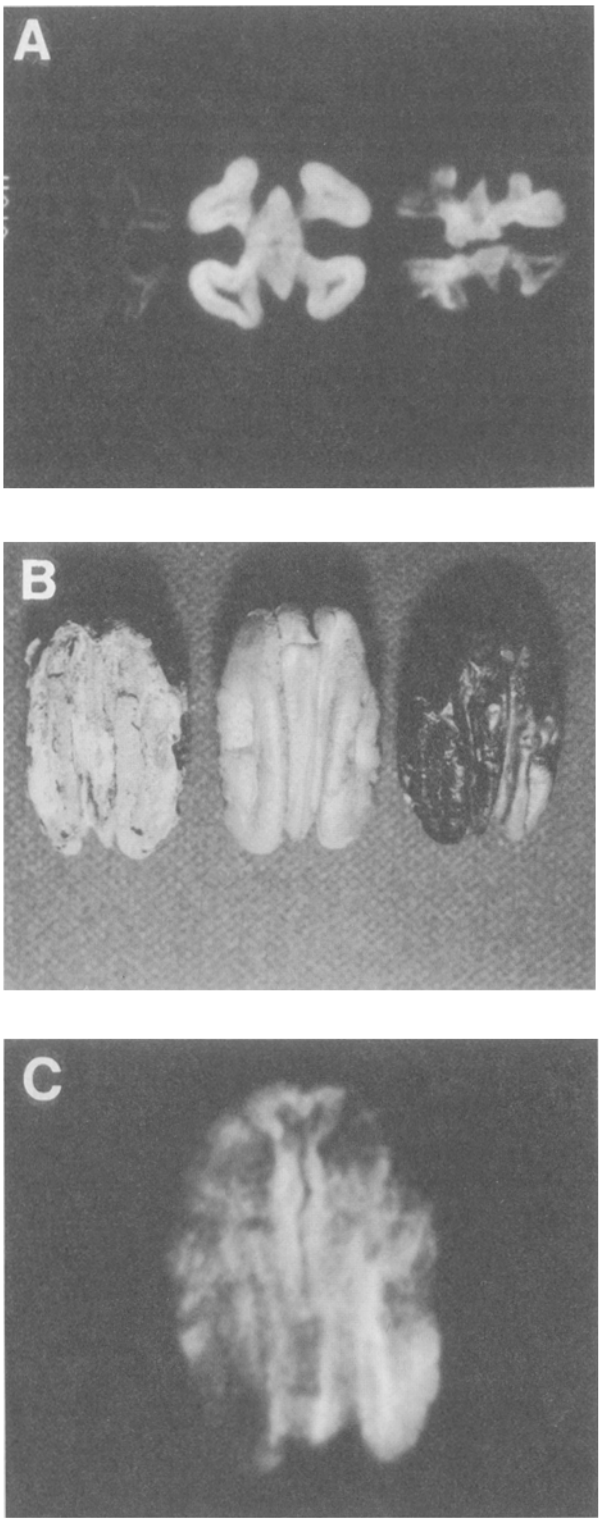

FIG. 3. A. Spin-echo magnetic resonance image of a transverse section, 2-mm thick, through air-dried pecan embryos showing a pecan rotted by the fungus *Phoma exocarpina* (left), a normal pecan (center) and a pecan damaged by the insect *Zerara viridula* (right). The dark area separating the cotyledons of the embryo at the right is the result of mechanical breakage of this embryo during handling. B. Photograph of the same embryos shown above. C. Spin-echo image of 1 mm-thick slice within the plane of the cotyledon seen to the right in Figure 2B.

CSI, as applied here, images the entire thickness of the sample, and is thus influenced by sample topography; the relatively planar shape of pecan cotyledons tends to reduce this problem, as would prior manual sectioning of thicker samples. A modified CSI technique that has been used to image lipid distributions in clove pedicels, fennel fruits and orange albido (17) enables selection of ST comparable to that with SEI, but it still requires long imaging times.

ACKNOWLEDGMENTS

We thank Dr. Alvin Rogers for identification of *P. exocarpina*, and Dr. Gale Harris for his helpful technical suggestions.

REFERENCES

1. Bottomley, P.A., H.H. Rogers and T.H. Foster, *Proc. Natl. Acad. Sci. USA 83*:87 (1986).
2. Brown, J.M., G.A. Johnson and P.J. Kramer, *Plant Physiol. 82*:1158 (1986).
3. Chen, P., and R. Kauter, *Am. Soc. Agric. Engr.*, Paper No. 88-6592, Dec. 13-16, 1988.
4. Hall, L.D., V. Rajanayagam, W.A. Stewart and P.R. Steiner, *Can. J. For. Res. 16*:423 (1986).
5. Johnson, G.A., J. Brown and P.J. Kramer, *Proc. Natl. Acad. Sci. USA 84*:2752 (1987).
6. MacFall, J.S., G.A. Johnson and P.J. Kramer, *Ibid. 87*:1203 (1990).
7. Rogers, H.H., and P.A. Bottomley, *Agron. J. 79*:957 (1987).
8. Wang, C.Y., and P.C. Wang, *Hort. Sci. 24*:106 (1989).
9. Watt, B.K., *Metabolism,* edited by P.L. Altman, and D.S. Dittmer, Federation of American Society of Experimental Biology, Bethesda, 1968, p. 30.
10. Lauterbur, P.C., *Pure Appl. Chem. 40*:149 (1974).
11. Brown, T.R., B.M. Kincaid and K. Ugurbil, *Proc. Natl. Acad. Sci. USA 79*:3523 (1982).
12. Wehrli, F.W., J.R. MacFall and T.H. Newton, in *Advanced Imaging Techniques*, edited by T.H. Newton, and D.G. Potts, Clavadel Press, San Anselmo, 1983, pp. 87-117.
13. Madden, G.D., *Pecan Quart. 6*:23 (1972).
14. Fullerton, G.D., in *Magnetic Resonance Imaging*, edited by D.D. Stark, and W.G., Bradley, Jr., The C. V. Mosby Co., St. Louis, 1988, pp. 36-55.
15. Yatsu, L.Y., and T.J. Jacks, *Plant Physiol. 49*:937 (1972).
16. Gassner, G., and J.A.B. Lohman, *Proc. Natl. Acad. Sci. USA 84*:5297 (1987).
17. Pope, J.M., H. Rumpel, W. Kuhn, R. Walker, D. Leach and V. Sarafis, *Magnetic Resonance Imaging 9*:357 (1991).

[Received March 16, 1993; accepted September 16, 1993]